Energy Conversion and Management 346 (2025) 120489

Contents lists available at ScienceDirect

Energy Conversion and Management

journal homepage: www.elsevier.com/locate/enconman

Research Paper

Modeling and simulation of thermal management in battery electric rail vehicles for the sizing of thermal storage systems

Steffen Wieser [a,*], Lucas Naveau [a], Werner Kraft [a], Ruth Arregi Beristain [b], Armando Anson [b]

[a] Institute of Vehicle Concepts, German Aerospace Center (DLR), Stuttgart, Germany
[b] Construcciones y Auxiliar de Ferrocarriles (CAF), Beasain, Spain

ARTICLE INFO

Keywords:
Heating
HVAC
Thermal energy demand
Cabin model
BEMU
Public transport

ABSTRACT

The need for sustainable public passenger transport has led to an increase in the number of battery electric rail vehicles in development and operation. Nevertheless, the energy demand for the heating of the passenger cabin is provided by the battery and leads to limited range, especially at low ambient temperatures. Thermal storage systems offer an innovative possibility to reduce energy demand for heating from the battery. Therefore, the presented paper studies the requirements for such thermal storage systems in battery electric rail vehicles. A thermal car body model is developed in Python and the thermal energy demand in battery electric vehicle operation is simulated. Scenarios and boundary conditions for environment, track, vehicle and HVAC (heating, ventilation, air conditioning) control parameters are specified based on current codes and standards for rail vehicles. The thermal power demand is up to 48 kW in summer and 92 kW in winter for the presented scenario in climate zone III according to DIN EN 14750. The required size of a thermal storage system is between 52 kWh and 255 kWh. Overall, the application of these systems leads to an increased rail vehicle range of up to 5.6 %, which also leads to greater flexibility of the vehicles as they are more resilient against disturbances in daily operation.

Nomenclature

APS	Auxiliary Power System
BEMU	Battery Electric Multiple Unit
CAF	Construcciones y Auxiliar de Ferrocarriles
COP	Coefficient of Performance
DCDC	Direct Current, Direct Current
DLR	German Aerospace Center
EU	European Union
FP	Flagship Project
HEMU	Hydrogen Electric Multiple Unit
HVAC	Heating, Ventilation, Air Conditioning
ICE	Inter-City Express (German high-speed train)
mPCM	metallic Phase Change Material
OESS	On-board Energy Storage System
OP	Operating Point
OPK	Operating Point Kalmar (local)
PC	Power Car
TCBM	Thermal Car Body Model
TGV	Train à Grande Vitesse (French high-speed train)

Symbols

α_i	Heat transfer coefficient for convection inside
α_o	Heat transfer coefficient for convection outside
$\alpha_{o,wall}$	Heat transfer coefficient for convection at outer wall
$\alpha_{o,window}$	Heat transfer coefficient for convection at outer window
λ	Thermal conductivity
A	Area
c_P	Specific heat capacity at constant pressure
C	Heat capacity
d	Thickness
$E_{cool,therm,a}$	Annual thermal energy demand for cooling
$E_{heat,therm,a}$	Annual thermal energy demand for heating
Δh_{cb}	Change of specific enthalpy of the air in the cabin over a time step
$h_{cb,t}$	Specific enthalpy of the air in the cabin at time step t
$h_{cb,t+1}$	Specific enthalpy of the air in the cabin at time step t + 1
h_v	Vaporization enthalpy of water
H	Absolute enthalpy
m_{cb}	Mass of air in the cabin
$m_{w,cb}$	Mass of water in the cabin
$\dot{m}_{in}$	Mass flow of air entering the cabin

(*continued on next page*)

* Corresponding author.
E-mail address: Steffen.Wieser@dlr.de (S. Wieser).

https://doi.org/10.1016/j.enconman.2025.120489
Received 13 June 2025; Received in revised form 26 August 2025; Accepted 4 September 2025
Available online 13 September 2025
0196-8904/© 2025 The Authors. Published by Elsevier Ltd. This is an open access article under the CC BY license (http://creativecommons.org/licenses/by/4.0/).

Symbols (*continued*)

$\dot{m}_{Pass}$	Mass flow of water emitted by the passengers
$\dot{m}_{out}$	Mass flow of air leaving the cabin
$P_{cool,therm,avg}$	Thermal power for cooling, averaged over the cycle
$P_{cool,lat}$	Thermal power for latent cooling
$P_{cool,sens}$	Thermal power for sensible cooling
$P_{heat,sens}$	Thermal power for sensible heating
$P_{heat,therm,avg}$	Thermal power for heating, averaged over the cycle
P_{total}	Total power
$P_{total,therm}$	Total thermal power
$\dot{Q}_{cb,total}$	Total heat flow entering or leaving the cabin
$\dot{Q}_{Cond,i}$	Heat flow from conduction at inside
$\dot{Q}_{Cond,o}$	Heat flow from conduction at outside
$\dot{Q}_{Conv,i}$	Heat flow from convection at inside
$\dot{Q}_{Conv,o}$	Heat flow from convection at outside
$\dot{Q}_{cool,therm}$	Heat flow cooling
$\dot{Q}_{El}$	Heat flow from electrical heating
$\dot{Q}_{heat,therm}$	Heat flow heating
$\dot{Q}_{in}$	Heat flow entering the cabin with entering air
$\dot{Q}_{out}$	Heat flow leaving the cabin with leaving air
$\dot{Q}_{Pass}$	Heat flow from passengers
$\dot{Q}_{Pass,sens}$	Sensible heat flow from passengers
$\dot{Q}_{Pass,lat}$	Latent heat flow from passengers
$\dot{Q}_{Rad}$	Heat flow from radiation
$\dot{Q}_{Rad,abs}$	Heat flow from radiation absorbed by the wall
$\dot{Q}_{Rad,em}$	Heat flow from radiation emitted by the wall
$\dot{Q}_{Rad,win}$	Heat flow from radiation transmitted by the window
$\dot{Q}_{Trp}$	Heat flow through heat transport
t	Time
Δt	Change of time / time step
T	Temperature
T_{amb}	Ambient temperature
T_{cb}	Temperature in cabin
$T_{cb,ref}$	Reference setpoint temperature in cabin
T_S	Temperature at melting point
$T_{Surf,i}$	Surface temperature inside
$T_{Surf,o}$	Surface temperature outside
T_t	Temperature at time step t
T_{t+1}	Temperature at time step t + 1
v	Velocity
$\dot{V}_{CA}$	Volume flow of circulating air
$\dot{V}_{CEA}$	Volume flow of cabin entering air
$\dot{V}_{FA}$	Volume flow of fresh air
$\dot{V}_{fresh,P,sp}$	Setpoint volume flow of fresh air
$\dot{V}_{MA}$	Volume flow of mixed air of recirculating air and fresh air
Δx_{cb}	Change of absolute humidity over a time step
$x_{cb,t+1}$	Absolute humidity in the cabin at time step t + 1
x_{in}	Absolute humidity of the air entering the cabin
x_{out}	Absolute humidity of the air leaving the cabin

1. Introduction

Battery electric rail vehicles are currently becoming a part of sustainable passenger rail transport. The following chapter introduces the specifications of the vehicles and states the current projects of the implementation of networks with battery electric rail vehicles. The thermal management system with special focus on heating, ventilation and air conditioning (HVAC) is presented as well as the state-of-the-art of thermal storage application in vehicles.

1.1. Battery electric rail vehicles

The EU rail network sums up to over 200.000 km of tracks, of which 85.000 km, corresponding to 43 %, are not electrified with a catenary. Germany, as a central European country, has the biggest share of the EU rail network with 38.000 km of tracks overall and a share of track electrification of 45 % [1]. The sections without catenary are mainly used by regional passenger transport. High-speed rail vehicles such as the TGV or ICE only use electrified sections with catenary. Nevertheless, the non-electrified sections lead to 25,000 diesel rail vehicles in operation in Europe compared to 60,000 rail vehicles overall [2]. For sustainable rail transport, diesel vehicles need to be replaced by vehicles that use renewable energy sources. Battery electric or hydrogen electric multiple units (BEMU/HEMU) are possible solutions for this.

BEMUs are especially suitable on tracks which are partly electrified, e.g. around stations. As these track sections are mainly part of the regional passenger transport, this is the main use-case for BEMUs. Several BEMUs were developed in the last years and a first passenger operation was tested in a project starting 2016 from Alstom [3]. Currently, there are several BEMUs commercially available, e.g. Alstom Coradia Continental BEMU, CAF Civity, Siemens Mireo Plus B or Stadler Flirt Akku. As first network for battery electric passenger transport, the NAH.SH network started operation in 2024 with over 50 Stadler Flirt Akku vehicles. Other networks will follow soon such as the Irish Rail DART network or the Pfalznetz in Germany [4]. Also, several new networks are tested for BEMU suitability e.g. in Italy [5].

The power supply of the BEMUs consists of the batteries as on-board energy storage system and a pantograph for battery charging and external power supply from the catenary [6]. Battery capacity in current BEMUs is up to 700 kWh which enables a range between 80 km and 120 km [7]. This range needs to be ensured even under the highest energy demand, which occurs on days with the lowest or highest ambient temperature in operation.

To increase the range of the vehicles, optimization potentials for the reduction of energy demand from the battery are studied in several publications. In [8], the energy demand is reduced with the implementation of energy-optimized timetables, energy-efficient driving strategies, improved control of comfort functions and wayside energy storage devices. In [9], the speed profile, power control and battery charging are optimized with the condition of charge sustaining operation. In [10], an optimization is performed to identify the trajectory with the minimal energy demand. Several tools for energy simulation of rail vehicles are developed such as in [11], where the sensitivity of energy demand is evaluated with respect to the selected design variables of the vehicles. On infrastructure side, the specific existing electrification and line lengths are analyzed to show that the BEMU operation can lead to a significant cost reduction compared to a full electrification [12]. For a sustainable rail transport, all options for reduction of emissions need to be discussed with regard of the specific local boundary conditions, as HEMU, BEMU, full electrification or hydrated vegetable oils can deliver suitable solutions [13]. In [14], different key performance indicators for optimal energy management of urban rail systems are defined, which include CO_2 emissions and vehicle auxiliaries. The effects of ambient temperature on electric vehicle range are studied in [15] and it is shown that the HVAC energy consumption has the greatest impact. Overall, it can be seen that a lot of optimizations aim to reduce the energy demand from the battery and that the energy demand from the HVAC system has a significant impact on the range of the vehicles, especially in environmental conditions with high or low ambient temperatures.

1.2. HVAC and thermal management systems in rail vehicles

HVAC systems in rail vehicles provide thermal comfort to the passengers as they condition the cabin inlet air. Circulating air is mixed with fresh air and the resulting airflow is heated or cooled before it enters the cabin. The conditions for thermal comfort are defined in DIN EN 14750 for rail vehicles in regional rail passenger transport [16]. DIN EN 13129 specifies these parameters for the high-speed rail passenger transport [17]. Standardized operating points (OP) for rail passenger transport are given in DIN EN 50591, which consist of passenger rate, solar radiation, ambient temperature and humidity [18].

Steady-state or dynamic models, or even combinations of these two approaches, can be used to calculate energy demand in HVAC systems [19]. In [20], the cabin of a rail vehicle is modeled with a linear dynamic discrete time system. In addition, parameter sets for heat capacities in rail vehicles are provided. In [21], the thermal behavior is modeled with

a mono-zonal model and the results show that the energy demand for the cabin and the battery temperature severely limit the range of battery electric vehicles. For the measurement of thermal energy demand and thermal comfort in trains, experiments with thermal passenger manikins can be used to imitate passengers [22]. The presented studies demonstrate that investigations of HVAC systems are performed either in experiments or simulations.

A lot of HVAC-related work is also about the integrated thermal management of vehicles, as the heat flow in different heat sources and sinks like the cabin or the battery is optimized in a holistic approach [23]. With a hierarchical multi-horizon model predictive control, the battery degradation and total costs with such an integrated thermal management are presented in [24]. The integrated thermal management approach is especially feasible if a heat pump absorbs heat from the battery during discharging or charging processes and the heat is then used for cabin heating [25]. Even with heat pump application in a passenger vehicle at −17 °C the range is reduced by 52 % compared to moderate temperature according to [26]. If waste heat recovery is used in addition to the heat pump, range is reduced by 37 %. Energy consumption through heating can be reduced if waste heat is used, as presented in a three-heat source segmented heating control strategy in [27]. As heat sources, e-motor, air and positive temperature coefficient heaters are used. Waste heat recovery in an integrated design, based on solenoid and four-way reversing valves, is studied in [28]. Different coupling relationships between the battery chiller and the cabin heat exchanger define the different states in the integrated thermal management. The stated references show that it is important to design the thermal management of electric vehicles with holistic integrated approaches that combine energy storage and passenger cabin.

For the heat transfer in HVAC systems, refrigerants are one key component. Currently used refrigerants will be replaced in the future with lower global warming potential versions as specified in EU-regulation 2024/573. In [29], CO_2 is used as refrigerant in trains and heat is provided in heat pump application down to an ambient temperature of −20 °C. For CO_2, the high pressure is critical for the gas leading components. In [30], a control algorithm is presented for the transcritical CO_2 cycle of a train HVAC system, which provides a coefficient of performance (COP) between 1.5 and 2.7 at 45 °C to 35 °C. Alternatively, propane can be used as natural refrigerant. For safety reasons, double loops are often applied, but single loops provide up to 50 % higher COP according to [31].

Regardless of the refrigerant, the energy demand of HVAC has a significant influence on the range and autonomy of vehicles. In [32], it is presented that for a train compartment, the cooling load in ventilation has the highest share in the overall cooling load. Conduction and radiation cooling loads are lower. A combined electric-thermal collaborative energy management strategy for a passenger train is proposed in [33] to optimize on-board power distribution between traction and auxiliary power. In [34], a collaborative energy management strategy based on a soft actor-critic algorithm optimizes the thermal safety of the battery and the cabin thermal comfort. For buses in real driving cycles in winter, the energy consumption of the auxiliaries sums up to 8 % of the total consumption, whereas electric heaters and compressors have a share of 60 % of this [35]. New HVAC technologies like metal hydride based air conditioning are also developed to reduce HVAC energy demand and studied for rail requirements [36]. Adsorption air conditioning systems are studied with rail requirements to reduce energy demand by using waste heat [37]. In [38], an optimized operation strategy for BEMUs is developed, which uses catenary-dependent temperature set points in the cabin to reduce energy demand from the battery. A case study of commuter trains in Sweden shows that HVAC demand can be decreased by 34 % if a parking mode is activated and by 43 % if a heat pump is applied in the trains [39].

The comparison of the HVAC studies shows that lumped parameter models are a suitable approach to model energy demand in vehicles. Also, a lot of optimization potentials are discussed which reduce HVAC energy demand from the battery. Alternative energy storage options such as thermal storage systems are a possible solution to contribute to this optimization.

1.3. Thermal storage systems as energy storage

Thermal storage systems are an option of energy storage. They are considered in stationary and mobile applications. In stationary use cases, they can be used to stabilize the local power grid [40]. Especially in combination with renewable energies, they provide optimization potential, also in the energy management of buildings [41]. They can be used to optimize energy demand for data centers in combination with waste heat recovery [42]. In the energy sector, thermal storage systems can be used to increase the performance of compressed air energy storage in caverns [43] or in combination with geothermal energy [44]. For mobile applications, thermal storages have been discussed as part of the energy management in passenger vehicles. They can cover a large share of the heating demand which occurs in passenger vehicles and increase the range of the vehicles [45]. For passenger cars they can increase the range of the vehicle by up to 27 % [46]. Even higher potentials for the use of thermal storage systems are discussed in bus applications. Buses have a higher demand in thermal energy because of the large cabin and higher cost for the battery system than passenger vehicles [47]. For rail vehicles, a study for the thermal storage application was performed for a reference track in Germany, which shows high potential for the reduction of energy demand and total cost of ownership in the battery system [48].

As thermal storage material in stationary applications, salt is often used because of its low cost and high availability. For mobile applications, metallic phase change materials (mPCM) are considered because of potentially higher energy densities [49]. As part of the phase change, latent heat can be stored additional to the sensible heat. For stationary applications, the storage of waste heat in the thermal storage systems from the surrounding energy management system is discussed [50]. In mobile applications, an electrical charging systems and processes are developed as the temperature level of waste heat from battery systems is relatively low [51].

The comparison of various studies about thermal storage systems shows that they are an established technology, particularly in stationary applications. However, there are clear research gaps for the application in mobility sector and especially in rail vehicles, as the requirements and effects of thermal storage have hardly been investigated and described in these research areas.

1.4. Aims of this study and work novelty

The previous sections describe the challenges for the operation of battery electric rail vehicles and their thermal management resulting from the high thermal energy demand for HVAC. The energy demand for HVAC is higher compared to other vehicle applications like passenger cars or buses as the size of the cabin is larger. The current thermal management systems provide the energy demand for HVAC from the battery. Solutions which reduce this energy demand from the battery are necessary to increase the share of battery electric rail vehicles in public passenger transport as it limits the range and flexibility of the vehicles in operation. For mobile application, several references in literature can be found which discuss optimization potentials to reduce energy demand in HVAC and at the battery. For rail vehicles, only a few references are available which discuss this topic even though the demand for sustainable rail passenger transport is increasing. Thermal storage systems are a promising technology to reduce energy demand at the battery but for the application in battery electric rail vehicles, there is a research gap of references, which discuss the requirements for these systems in different climate zones of operation. Thermal storage systems need to be integrated in the thermal management and sized properly to supply the energy demand for HVAC and reduce energy demand from the battery.

As currently battery electric rail vehicles are not equipped with thermal storage systems, the development process of this new component in the thermal management system starts with the definition of requirements and suitable sizing options. Therefore, the presented work addresses the following research question: What are the requirements for thermal storage systems in the application of battery electric trains and which advantages occur with the integration of thermal storage systems in the on-board energy storage?

The contributions from this work to address the presented research gap are the sized thermal storage systems in terms of energy content as well as charging and discharging rates for the application in battery electric rail vehicles. Accordingly, the objective of this study is to model and simulate the thermal energy demand in battery electric rail vehicles and define requirements and sizing options of thermal storage systems based on simulation results. In addition, the effects on vehicle level will be evaluated based on the increase in range and therefore also flexibility in vehicle operation.

2. Methodical approach – Parametrization and modeling of HVAC in battery electric rail vehicles

For the definition of requirements for thermal storages in battery electric rail vehicles, the thermal energy demand is calculated with a thermal car body model. The model is parameterized with a reference vehicle and uses the vehicle trajectory and environmental conditions as inputs. The model setup, input parameters and model validation are presented in the following chapter.

2.1. Thermal car body model

A thermal car body model (TCBM) was set up in Python for the investigation of the thermal energy demand in rail vehicles. The TCBM models the conditioning of the air for the cooling and heating of the passenger cabin and the corresponding thermal energy demand. The scope of the model is presented in Fig. 1.

In the mixing chamber the fresh airflow $\dot{V}_{FA}$ and the circulating airflow $\dot{V}_{CA}$ are mixed and create the mixed airflow $\dot{V}_{MA}$, which enters the HVAC system. In there, the air is heated with the thermal heat flow $\dot{Q}_{heat,therm}$ for heating cases or cooled with the extraction of the thermal heat flow $\dot{Q}_{cool,therm}$. All relevant volume and heat flows are summarized in Fig. 2. The conditioned airflow $\dot{V}_{CEA}$ enters the cabin and is one term of the first law of thermodynamics for the cabin, as presented in equation (1). In there, the enthalpy change $\frac{dH}{dt}$ of the air in the cabin is calculated based on the heat transport from convection and conduction $\dot{Q}_{Trp}$, heat flow from radiation $\dot{Q}_{Rad}$, heat flow from passengers $\dot{Q}_{Pass}$, heat flow from electrical heating in the cabin $\dot{Q}_{El}$ as well as mass flow $\dot{m}_{in/Pass/out}$ and enthalpy $h_{in/Pass/out}$ from inlet, passengers and outlet. If the time step Δt is small enough, the change in specific enthalpy of the air in the cabin Δh_{cb} can be calculated based on equation (2) with the mass of air in the cabin m_{cb}. The enthalpy of the air in the cabin in the next time step $h_{cb,t+1}$ is then calculated by the addition of the enthalpy of the air in the cabin in the current time step $h_{cb,t}$ and the change in specific enthalpy of the air in the cabin Δh_{cb} as presented in equation (3).

$$\frac{dH}{dt} = \dot{Q}_{Trp} + \dot{Q}_{Rad} + \dot{Q}_{Pass} + \dot{Q}_{El} + \dot{m}_{in}\cdot h_{in} + \dot{m}_{Pass}\cdot h_{Pass} - \dot{m}_{out}\cdot h_{out} \tag{1}$$

$$\Delta h_{cb} = \frac{1}{m_{cb}}\cdot\frac{dH}{dt}\cdot\Delta t \tag{2}$$

$$h_{cb,t+1} = h_{cb,t} + \Delta h_{cb} \tag{3}$$

To calculate the humidity in the cabin, the change of the mass of water in the cabin $m_{w,cb}$ is calculated with equation (4) based on the absolute humidity $x_{in/out}$, which describes the content of water in the air. The amount of water entered by the passengers is described by equation (5) through the ratio of the latent heat flow of the passengers $\dot{Q}_{Pass,lat}$, based on DIN EN 14750 and the enthalpy of evaporation h_v. The change of absolute humidity of the air in the cabin Δx_{cb} is calculated with equation (6) and the absolute humidity of the air in the cabin for every time step $x_{cb,t+1}$ with equation (7).

$$\frac{dm_{w,cb}}{dt} = \dot{m}_{in}\cdot x_{in} + \dot{m}_{Pass} - \dot{m}_{out}\cdot x_{out} \tag{4}$$

$$\dot{m}_{Pass} = \frac{\dot{Q}_{Pass,lat}}{h_v} \tag{5}$$

$$\Delta x_{cb} = \frac{1}{m_{cb}}\cdot\frac{dm_{w,cb}}{dt}\cdot\Delta t \tag{6}$$

$$x_{cb,t+1} = x_{cb,t} + \Delta x_{cb} \tag{7}$$

Heat transfer is modeled through the wall and the window of the cabin. The change of the temperature in the wall is modeled through the ratio between heat flow due to conduction in the inner respectively outer wall $\dot{Q}_{Cond,i/o}$ and the heat capacity of the wall C, according to equation (8). The temperature in the wall for every time step T_{t+1} is calculated with equation (9). The first law of thermodynamics for the inner and outer surface of the cabin wall is presented in equation (10). In there, the heat flows for conduction $\dot{Q}_{Cond,i/o}$, convection $\dot{Q}_{Conv,i/o}$ and radiation $\dot{Q}_{Rad,abs/em}$ are evaluated. This equation is solved for the calculation of the surface temperature on the inside and outside $T_{Surf,i/o}$ in equation (11). Heat flow for conduction is modeled according to equation (12) and heat flow for convection according to equation (13). The heat transfer coefficient on the outside $\alpha_{o,window}$ is modeled differently for windows and walls in dependency of the vehicle velocity according to equation (14) [52].

$$\frac{dT}{dt} = \frac{\dot{Q}_{Cond,i} + \dot{Q}_{Cond,o}}{C} \tag{8}$$

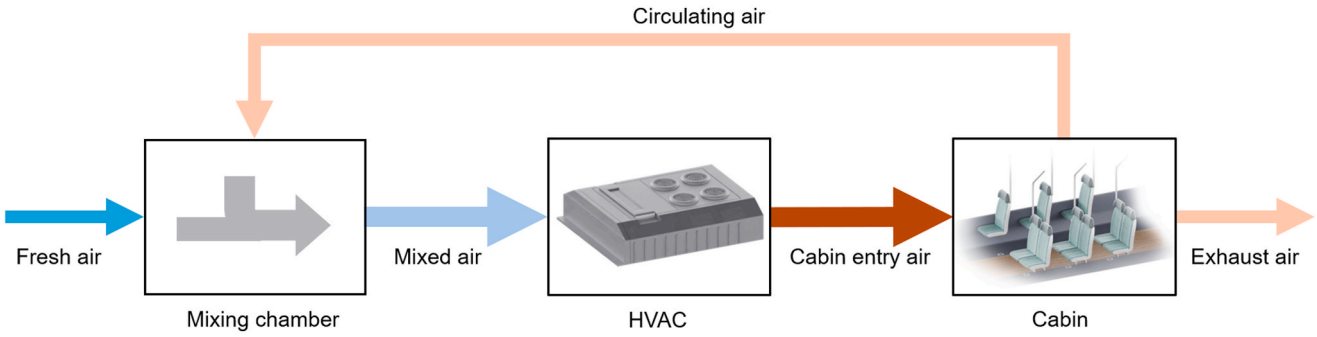

Fig. 1. Airflow and conditioning of air for the cabin in rail vehicles.

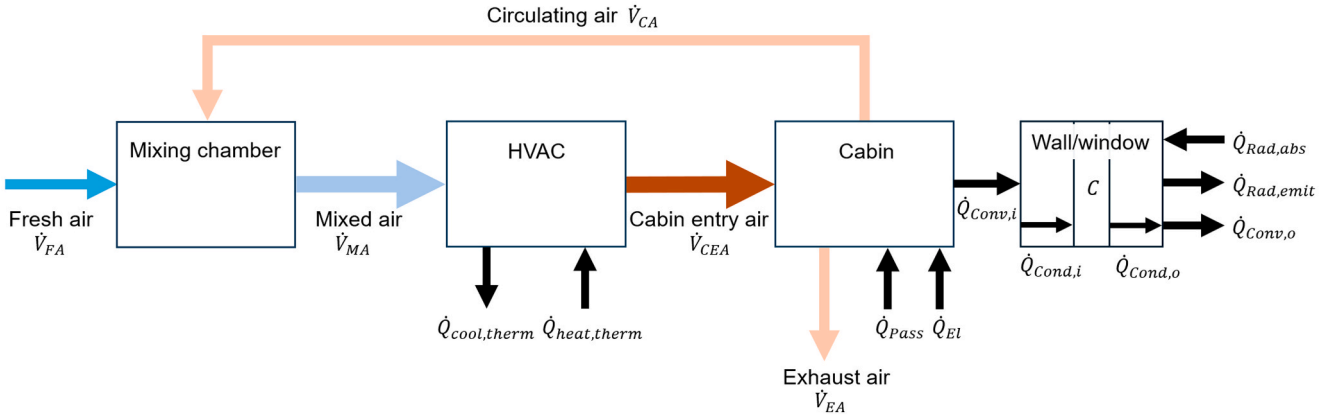

Fig. 2. Heat and volume flows of the thermal car body model.

$$T_{t+1} = T_t + \frac{\dot{Q}_{Cond,i,} + \dot{Q}_{Cond,o}}{C} \cdot \Delta t \tag{9}$$

$$\dot{Q}_{Cond,i/o} = \dot{Q}_{Conv,i/o} + \dot{Q}_{Rad,abs} - \dot{Q}_{Rad,em} \tag{10}$$

$$T_{Surf,i/o} = \frac{\frac{2\lambda}{d} \cdot A \cdot T + \alpha_{i/o} \cdot A \cdot T_{amb/cb} + \dot{Q}_{Rad,abs} - \dot{Q}_{Rad,em}}{\left(\frac{2\lambda}{d} + \alpha_{i/o}\right) \cdot A} \tag{11}$$

$$\dot{Q}_{Cond,i/o} = \frac{2\lambda}{d} \cdot A \cdot (T_{Surf,i/o} - T) \tag{12}$$

$$\dot{Q}_{Conv,i/o} = \alpha_{i/o} \cdot A \cdot (T_{cb/amb} - T_{Surf,i/o}) \tag{13}$$

$$\alpha_{o,window} = \begin{cases} 5,6 + 4 \cdot v \\ 7,12 \cdot v^{0,78} \end{cases} \alpha_{o,wall} = \begin{cases} 5,8 + 4 \cdot v \; for \; v < 5 \; m/s \\ 7,14 \cdot v^{0,78} \; for \; v \geq 5 \; m/s \end{cases} \tag{14}$$

All air volume flows, as well as the different states of the air and the heat transfer modes, are summarized as overview in Fig. 2. The heat transfer through the wall and window of the car body is displayed on the right. The model takes as input the parameter sets of the environment, the track and the vehicle and calculates the overall thermal energy demand for the heating and cooling of the passenger cabin.

For the control of temperature and humidity proportional–integral–derivative controllers are used. The temperature is regulated by controlling $\dot{Q}_{heat,therm}$ for heating cases and $\dot{Q}_{cool,therm}$ for cooling cases. The heat flows are regulated until the set point of the temperature in the cabin is reached. Humidity is controlled mainly in cooling cases as maximum values for humidity in the cabin are defined. Minimal values for the humidity in the cabin are not defined in rail-specific standards and not applied. For dehumidification, a sub-cooling and re-heating of the mixed air is simulated to keep the relative humidity in the cabin below the maximum values.

2.2. Thermal storage system

Thermal storage systems store thermal energy to separate moments of supply and demand of thermal power from each other. Thermal energy can be stored by increasing the temperature or changing the phase of a material, for example from solid to liquid state. The thermal energy is released by decreasing the temperature or by the reverse phase change, for example from liquid to solid state. The following section discusses the relevant principles and parameters of the thermal storage material and systems applied to the analysis of the presented work.

Metallic PCM have higher energy density than other thermal storage materials like salt or water as introduced in section 1.3. Exemplary gravimetric and volumetric energy density for thermal storage systems are nearly twice as high as in batteries, as presented in Table 1. In addition, the specific cost of the thermal storage is significantly lower than the specific cost for the battery. The high energy density and therefore, the low specific cost per kWh are a result of the high temperature in thermal storage with mPCM.

An alloy of aluminum and 12 % silicon in weight is used as reference material in this paper and was specified in earlier investigations in [49]. The alloy is an eutectic composition, which means that the phase change from liquid to solid state takes place at one specific eutectic temperature. The eutectic composition is very stable and has a low melting point compared to other compositions at around 577 °C, which makes it suitable for the application in thermal storage systems [49]. Small deviations in the alloy composition can lead to deviations in melting point, so that the phase change takes place in a small range of temperatures around the melting point for the exact eutectic composition. Depending on the size of the system small local temperature deviations in the material can occur, which can also lead to a slightly distributed phase change in the material in terms of time and location. In the charging process of the thermal storage system the sensible heat is stored in the solid state material until the temperature reaches the melting point (see Fig. 3 on the left). The temperature stays constant during the phase change and rises after the phase change is performed completely. The maximum temperature in operation for the reference system studied in this work is around 600 °C to 700 °C.

The setup of the reference thermal storage systems for this paper consists of storage material (mPCM), housing, insulation, electric heaters for charging and heat exchangers for discharging, as presented in Fig. 3 on the right. Electric heaters convert electrical energy in thermal energy with a coefficient of performance of 1 to charge the thermal storage system. This leads to an increase of stored thermal energy in the system as the temperature of the storage material rises and a phase change is performed from solid to liquid state. The system is discharged over heat exchangers which heat up the air for the cabin in their final stage. Thermal energy is extracted from the thermal storage material and absorbed by a heat transfer fluid which flows in the heat exchangers. The temperature in the thermal storage material is decreased and the phase change is performed from liquid to solid state. In this way, latent and sensible heat from the thermal storage material is used in the discharging process. Reduction in efficiency can occur through thermal losses during charging, storing or discharging, which would lead to a

Table 1
Battery and thermal storage energy density and specific cost [48,51].

	Thermal storage	Battery
Volumetric energy density	300 Wh/L	160 Wh/L
Gravimetric energy density	200 Wh/kg	90 Wh/kg
Specific cost	70 EUR/kWh	750 EUR/kWh

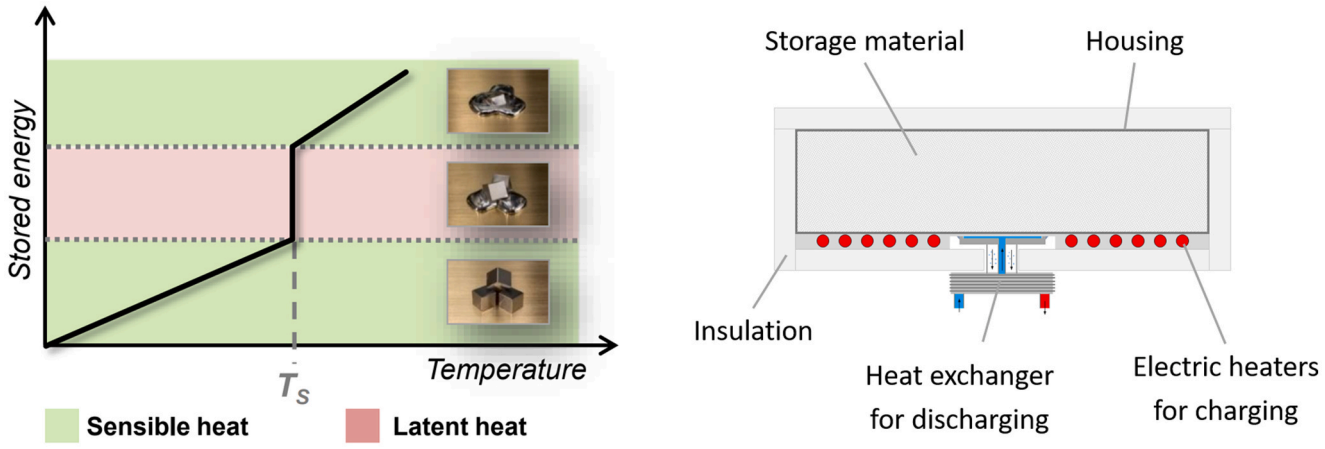

Fig. 3. Thermal storage with metallic phase change material – Phase change (left) and exemplary setup (right) [51].

heating of the cabin, if the thermal storage system is placed centrally in the vehicle. Therefore, an efficiency of 1 for the charging and discharging processes is assumed for the investigations of thermal storage system sizing in this work. As part of the operating strategy for thermal storage systems in a battery electric rail vehicle, the charging process takes place whenever catenary is available as an external power supply. The thermal storage system is discharged in sections without catenary to supply heat for the cabin, so that the energy does not have to be provided from the battery. The on-board energy storage system for the vehicle consists of the battery for electrical energy storage and the thermal storage system for thermal energy storage. Both systems are separated in the vehicle as they have different temperature levels of operation. The temperature levels of both components are controlled individually by their thermal management systems.

2.3. Parametrization of model and scenario

For the simulation of thermal energy demand with the TCBM to size thermal storage systems, environmental conditions, track, vehicle and HVAC control parameters need to be specified. The scenario simulated with the model in this study is the connection from Linköping to Kalmar in Sweden, operated by Trafikverket [53]. The corresponding input parameters are presented in the following section. The vehicle, track and timetable for this scenario are displayed in Fig. 4.

The reference vehicle is a 4-car battery electric multiple unit. Cars A1 and A2 are the first and last car with identical setups. Car B is a middle car which includes seats for passengers, whereas car PC is a power car, which includes batteries and power electronics. Car PC is connected to the other cars and passengers are able to walk through it, but there are no seats available. The track between Linköping and Kalmar is only electrified around the end stations. Non-electrified sections are marked as black in the bottom left of Fig. 4, whereas sections with catenary are marked in green. The charging of the vehicle only takes place in the end stations.

Environmental conditions for the reference scenario are provided by the weather and climate database Meteostat [54]. For the weather

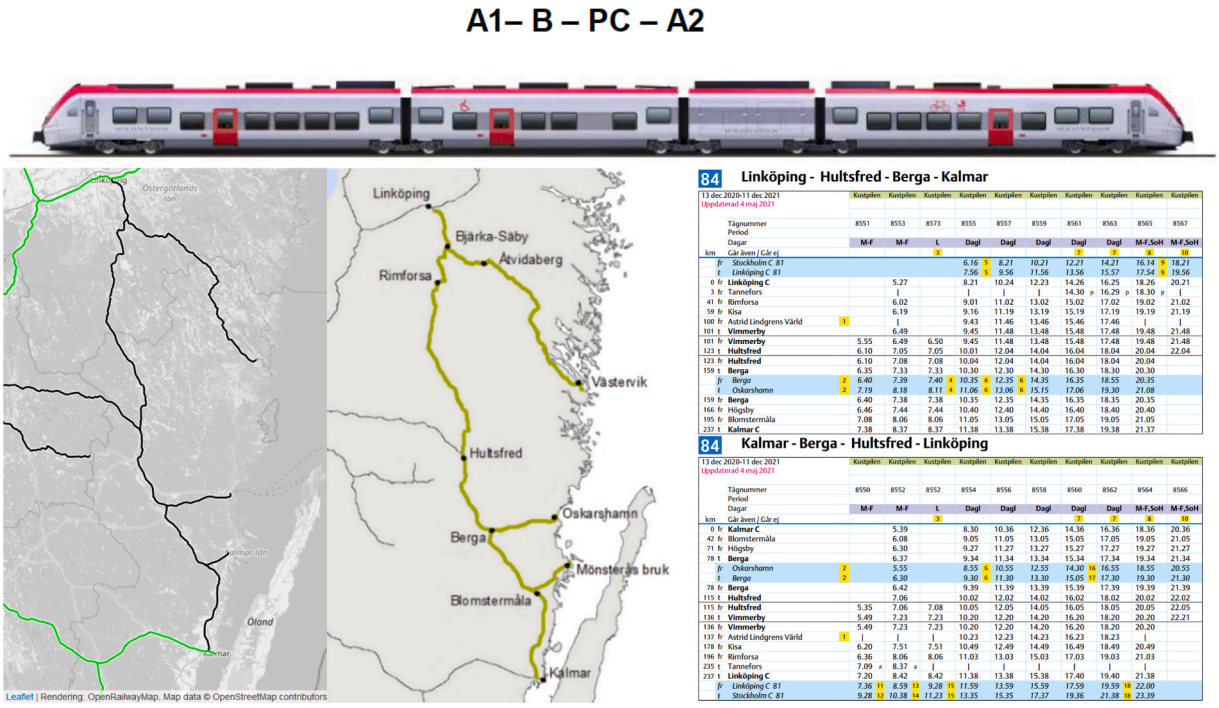

Fig. 4. Cars in the reference vehicle (top), OpenRailwayMap and Trafikverket map section (bottom left and mid) and timetable (bottom right) for the connection from Linköping to Kalmar [53].

station in Kalmar, the coldest temperature is −17.3 °C and the hottest temperature is 29.5 °C during the years 2019 to 2023. During the winter months, the hottest temperature recorded were 9 °C. These local temperature values are used for the definition of the operating points OPK01 to OPK06 in Table 2, combined with either a passenger rate of 100 % or 0 %.

Besides the local environmental conditions also the DIN EN 50591 defines 16 standardized operating points for rail vehicles. The OPs consist of a passenger rate, solar radiation, ambient temperature and humidity. OPs from DIN EN 50591 as well as the local OPs are used as input for the TCBM and summarized in Table 2. Some OPs in DIN EN 50591 have the same parameters such as OP01 and OP09. In the standard they are only differentiated because there are different yearly hours of operation for the different points. The standard distinguishes between climate zones I, II and III and varies the OPs for the different climate zones. In Table 2, the names indicated the climate zone, for example, climate zone I for OP06_I and climate zone II for OP06_II.

In addition to environmental conditions, the trajectory of the vehicle needs to be provided as input to the TCBM. The trajectory, as well as the inverter power, is plotted over the time in Fig. 5 for the track scenario from Linköping to Kalmar. After nearly 10,000 s and 236 km, the vehicle arrives in Kalmar and stops there for a charging process of the battery. At around 14,000 s, the vehicle starts its way back to Linköping and arrives there at around 24,000 s.

The reference vehicle presented in Fig. 4 has an overall length of 67.7 m, as presented in Table 3. The external surface of the passenger cabin is 633.5 m^2 and used as input in the TCBM, as the heat transfer with the environment is based on the external surface.

Control parameters in the HVAC system are the set points for the fresh air volume flow and the temperature in the passenger cabin. For rail vehicles, these set points are provided in the DIN EN 14750. In there, vehicle category R addresses a typical time between stops of 5–30 min, which is suitable for the presented reference scenario. The temperature and fresh air volume flow set points given for category R, vehicles according to DIN EN 14750, are presented in Fig. 6, in relation of the ambient temperature. For low ambient temperatures, the cabin temperature is set to 22 °C. If the ambient temperature is higher than 22 °C, also the cabin set temperature is increased. For ambient temperatures higher than 35 °C, the cabin temperature is set to 27 °C. The fresh air volume flow is set to 10 m^3/h/person for ambient temperatures lower than −15 °C. For higher ambient temperatures than −15 °C, it varies between 15 m^3/h/person and 20 m^3/h/person, as displayed in Fig. 6. For OPs with low passenger rate, a minimum fresh air volume flow of 4 m^3/h times the maximum passenger number is defined in DIN EN 14750 and applied in the TCBM. For category R, this maximum passenger number is equal to the number of seats in the vehicle.

Table 2
Operating points from DIN EN 50591 and operating points locally from Kalmar.

OP	Temperature in °C	Relative humidity in %	Passenger rate in %	Radiation in W/m^2
OP01/ OP09	−10	90	0	0
OP02	0	90	100	0
OP03	10	90	50	0
OP04	15	90	50	0
OP05	22	80	100	0
OP06_I/II	28	70	100	600
OP06_III	28	50	100	600
OP07_I	40	40	100	800
OP07_II	35	50	100	700
OP08_II	−20	90	0	0
OP08_III	−40	90	0	0
OP10/ OP14	0	90	0	0
OP11/ OP15	15	80	0	0
OP12	22	80	0	0
OP13_I	40	40	0	800
OP13_II	35	50	0	700
OP13_III	28	70	0	600
OP16	28	50	0	700
OPK01	−17	90	0	0
OPK02	−17	90	100	0
OPK03	9	90	0	0
OPK04	9	90	100	0
OPK05	29.5	90	0	600
OPK06	29.5	90	100	600

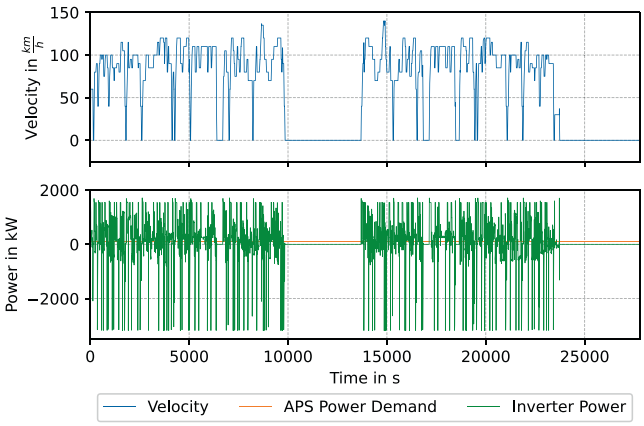

Fig. 5. Speed, auxiliary power and inverter power over distance for the track scenario with reference vehicle.

Table 3
Reference vehicle parameters.

Parameter	Value
Amount of car bodies	3 + 1 power car
Heating type	Resistance heating
Train length	67.7 m
A1/A2 car length	21.7 m
B car length	16.3 m
PC car length	8 m
External surface of passenger cabin	633.5 m^2

2.4. Validation of simulation results

The thermal HVAC power demand calculated by the presented Python TCBM is the key output parameter of the model and therefore used for validation. As a comparison, a TCBM Dymola model is used, which is validated with measurement data in [55] and presented in more detail in [56]. Fig. 7 shows the comparison of the thermal power demand for HVAC simulated with the Python model developed for this study and the validated Dymola model.

For the comparison, different OPs from DIN EN 50591 are used as input for the models. OP01, OP02, OP03, OP04 and OP08 are heating cases, whereas OP06 and OP07 are cooling cases. The power demand for validation is calculated in stationary operation for a parked vehicle without any velocity. The comparison between the two models shows that the Python model calculates a slightly higher power demand in the presented OPs. The absolute deviation shows a maximum of around 10 kW in OP7. The relative deviation shows a maximum deviation of 16 % in OP4 and OP7. Overall, the comparison demonstrates that the two models calculate similar results in heating and cooling cases. This leads to the fact that the developed Python model is valid to calculate the thermal energy demand for HVAC, which is used in the following analysis of thermal storages in battery electric rail vehicles.

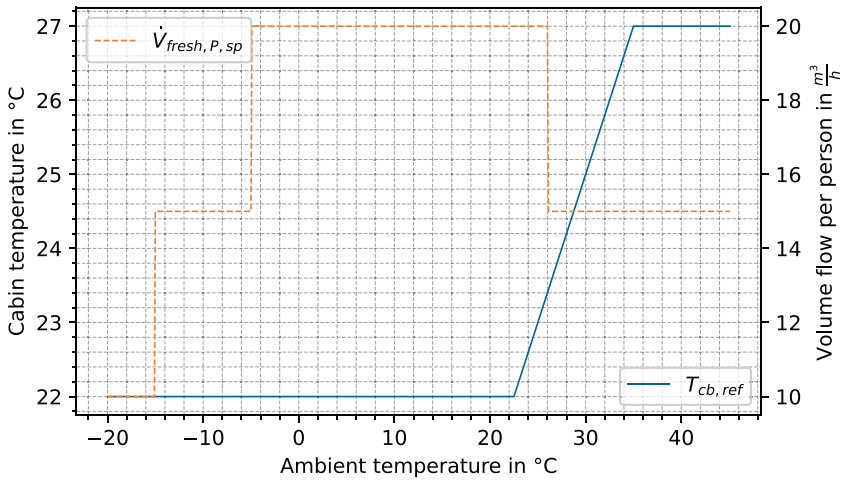

Fig. 6. Set temperature and fresh air volume flow rates in passenger compartment according to DIN EN 14750 [16].

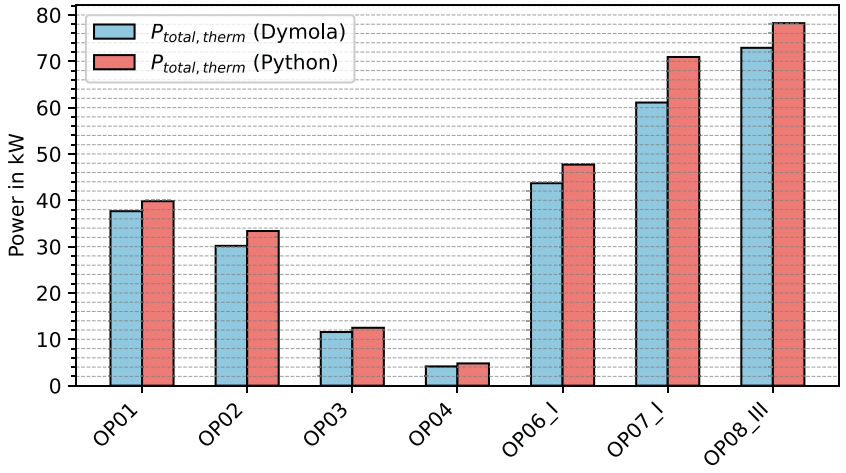

Fig. 7. Comparison of thermal power demand for HVAC for the reference vehicle from the Python model (red) and the validated Dymola model (blue) in different operating points.

3. Results – Thermal energy demand and thermal storage sizing

Simulations are performed with the presented TCBM and the described input parameters to calculate the thermal energy demand for HVAC in different scenarios. In the following chapter, this HVAC energy demand is presented, the requirements for thermal storage systems are concluded and the advantages of the application of such systems for battery electric rail vehicles are evaluated.

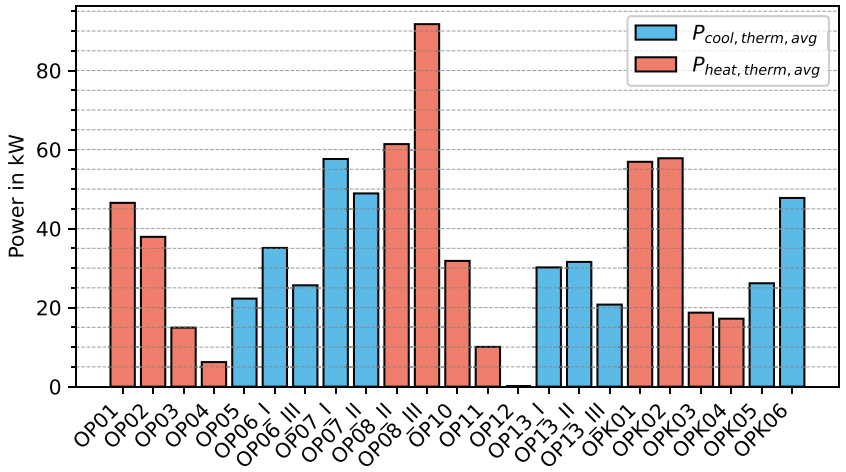

Fig. 8. Thermal power demand for HVAC of the reference vehicle in different operating points from Table 2.

3.1. Energy demand for HVAC in different operating points and climate zones

The thermal power demand for HVAC is calculated for the OPs from Table 2 and presented in Fig. 8. The highest power demand for heating is visible in OP8 for climate zone III with over 90 kW. For cooling, the highest power demand is from OP6 for climate zone I with 58 kW. The values are averaged over a half cycle of the driving profile presented in Fig. 5. For the local OPs, the highest power demand for heating reaches 58 kW in OPK02 and for cooling 48 kW in OPK06. The power demand of OPK06 is significantly higher as the one in OPK05, as in OPK06 the passenger rate is 100 %. This means that passengers emit humidity and heat, which increases the thermal energy demand for HVAC. For the heating cases, the power demand is similar for the passenger rate of 0 % and 100 %, e.g., in OPK01 and OPK02, even though the passengers emit additional heat. This is because a higher passenger rate also increases the fresh air volume flow, which needs to be conditioned before it is provided for the cabin, thus increasing the power demand.

The thermal power demand over a cycle is plotted on the bottom right in Fig. 9 for OP8_III, as this most demanding heating case is dimensioning for the sizing of thermal storage modules. Over the time, the fluctuations are low as the power demand changes between 90 kW and 92 kW. The changes are caused by the velocity-dependent change in the heat transfer coefficient on the outer surface of the car body. The humidity and temperature inside the cabin also show low fluctuations in the bottom left of Fig. 9, which indicates that the implemented humidity and temperature control work correctly and follow the prescribed set point values. The presented case of OP08_III is a heating case, which causes a low relative humidity of less than 1 %, as no humidification is included according to DIN EN 14750. Only for cooling cases dehumidification is implemented. OP08_III does not include passengers and radiation, therefore the terms of $\dot{Q}_{Rad}$ and $\dot{Q}_{Pass}$ in the plot on the top right in Fig. 9 are zero. Also, $\dot{Q}_{El}$ is zero as no additional electrical heating directly in the cabin is considered. For this case, the energy balance is based on the heat transport through walls and windows and heat flows $\dot{Q}_{in}$ and $\dot{Q}_{out}$ with the air entering and exiting the cabin.

The power demand for HVAC is different for the various OPs presented in Fig. 8. In addition to the OPs, DIN EN 50951 provides yearly operating hours for this OPs in different climate zones. Overall, 5,840 yearly operating hours are prescribed for the HVAC system of a rail vehicle in operation. With these yearly operating hours, a yearly thermal energy demand is calculated for the different climate zones and presented in Fig. 10. The red bars indicate the yearly thermal energy demand for heating cases, whereas the blue bars indicate energy demand for cooling. Climate zone I represents countries in southern Europe, climate zone II in central Europe and climate zone III in northern Europe. Fig. 10 shows that the yearly energy demand for cooling decreases from 58 MWh in climate zone I to 10 MWh in climate zone III. The energy demand for heating increases from under 50 MWh in climate zone I to 130 MWh in climate zone III. This evaluation shows that the yearly energy demand for heating is higher than for cooling. Especially in climate zone III, new solutions to reduce the energy demand for heating provided by the battery are necessary to improve the performance of battery electric vehicles in this climate zones. Thermal storages, which store heat at a high energy density and temperature are one option for this.

3.2. Requirements and sizing of thermal storage systems

Based on the thermal power demand for HVAC presented in Fig. 8, the requirements for thermal storage systems in the application of battery electric rail vehicles are defined. The requirements for the energy-based sizing of the thermal storage systems are the usable capacity as well as the charging and discharging power and C-rates. For the use-case presented in Fig. 4, different sizing options are presented with scenario A to E.

Scenario A corresponds to a sizing with the energy demand in the OP of the warmest winter temperature, which is OPK03 from Table 2. The sizing with the warmest winter temperature recorded locally leads to a usage rate of 100 % for the thermal storage system in every winter day. OPK03 gives an average power demand of 19 kW, which results in a thermal storage capacity of 52 kWh. Instead of the warmest winter temperature, the coldest winter temperature locally recorded is considered for scenario C. This scenario gives a thermal storage capacity that is able to provide all the heating demand of the vehicle throughout the whole winter. For OPK02, this is an average power demand of 58 kW, which results in a thermal storage capacity of 161 kWh. If the thermal storage system is not an independent additional system in the vehicle but replaces battery capacity in the vehicle, also the energy demand for cooling must be considered in the sizing process. This is done in scenario B. The average power demand for cooling in OPK06 of 48 kW results in an energy demand of 134 kWh over the cycle. As the cooling in rail vehicles is provided by a compression refrigeration system, the electrical energy demand is calculated with a COP = 3. This results in an electrical energy demand for cooling of 45 kWh, which is

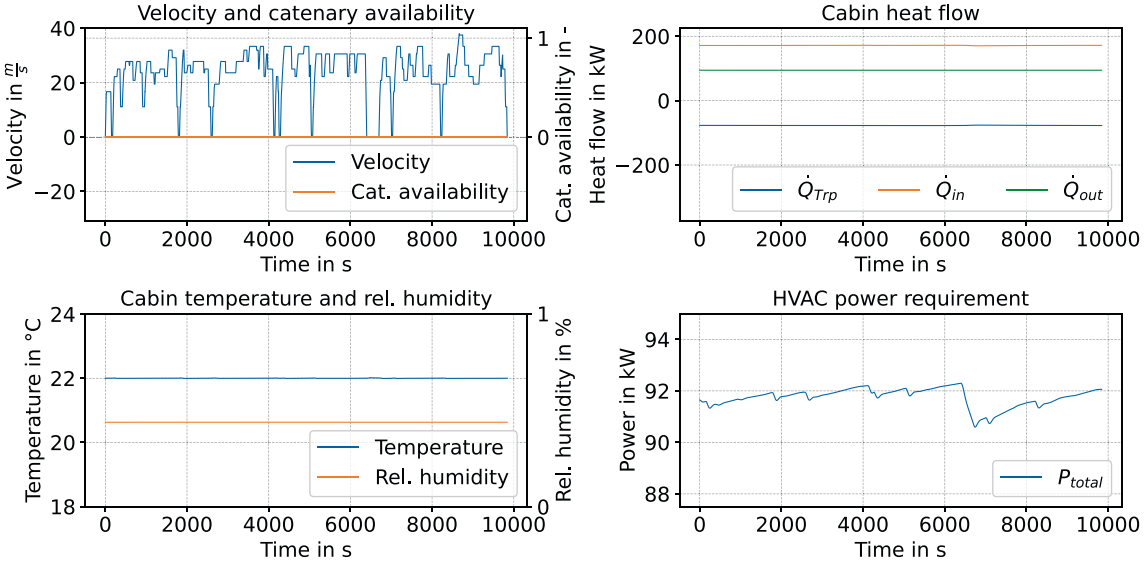

Fig. 9. Power demand and temperature of the reference vehicle over track scenario in OP8_III.

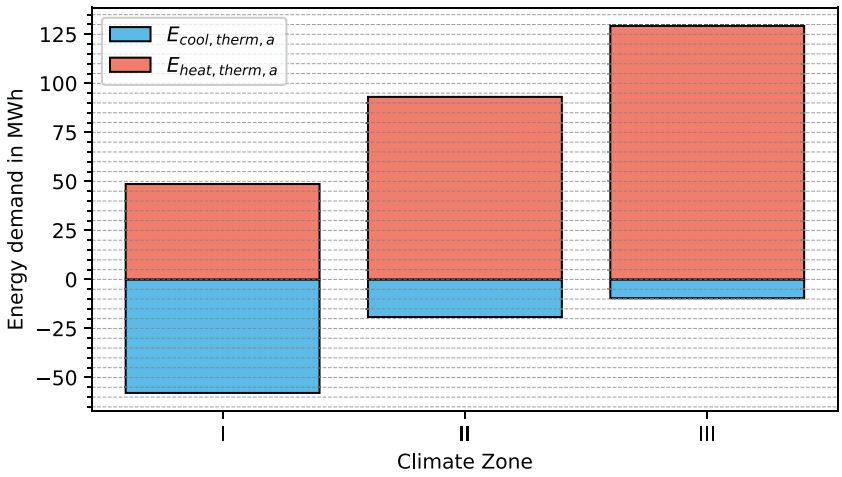

Fig. 10. Annual thermal energy demand of the reference vehicle for cooling (blue) and heating (red) in different climate zones.

subtracted from the 161 kWh for heating. For scenario B, this leads to a capacity of the thermal storage module of 116 kWh. In contrast to the local operating points, the thermal storage system can also be sized according to the normative operating points from DIN EN 50951 in the climate zone of operation. Consequently, scenario E is based in the average power demand of 92 kW from OP08_III and results in a capacity of the thermal storage system of 255 kWh. As with scenario B, the energy demand for cooling with 45 kWh is subtracted and results in a capacity of the thermal storage system of 210 kWh in scenario D. All scenarios with the concluded capacities are summarized in Fig. 11 on the left.

In addition to the capacity, also the charging and discharging rates are requirements for thermal storage systems. For the sizing, the maximum value of the charging and discharging rates are relevant. The discharging rate is depending on the maximum thermal power demand, which is 92 kW according to Fig. 8. For the scenarios A to E, this results in a maximum C-rate of discharge from 1.8 1/h to 0.38 1/h, as presented on the right of Fig. 11. The required charging rate of the thermal storage system is dependent on the stop time between different cycles. For the cycle of Fig. 5, a stop time of 1.1 h is defined, which corresponds to a C-rate of 0.9 1/h. For the scenarios A to E, this results in a required minimum average charging power by the thermal storage system during the charging process of 48 kW to 230 kW, as presented in the center of Fig. 11.

3.3. Advantages for vehicles with thermal storage systems

Hybrid on-board energy storage systems (OESS) for battery electric rail vehicles can be formed with a combination of thermal storages and batteries. The weight, volume and cost of the thermal storage systems needs to be considered in the vehicles design process. For the scenarios A to E from Fig. 11, the weight of the thermal storage system, based on the energy density from Table 1, is between 0.3 t and 1.3 t, as presented in Table 4. The volume of the thermal storage system is between 0.2 m^3 and 0.9 m^3, and the cost is between 3.6 k EUR and 17.9 k EUR. The values assumed in Table 1 are generalized characteristic values which may vary depending on the specific system design. The thermal storage system can be installed additionally to the battery sized for the vehicle and the corresponding time table if it is possible to add additional weight and if there is enough space. With the additional thermal storage system, the battery usage rate is reduced, which decreases degradation and therefore increases the lifetime of the battery system.

Alternatively, the thermal storage capacity can be used to replace battery capacity if the battery system is already sized in a way that no more weight or capacity can be added to the vehicle. A hybrid OESS, where some of the battery capacity, is replaced by thermal storage capacity has a higher gravimetric and volumetric energy density and lower specific cost than a stand-alone battery. For rail vehicles, weight is often a limiting factor as the maximum axle load cannot be exceeded [5]. For

Table 4
Amount of energy, weight, volume and cost for different sizes of thermal storages.

Scenario	Thermal storage capacity	Weight in t	Volume in m^3	Cost in k EUR	Additional energy in %
A	52 kWh	0.3	0.2	3.6	1.1
B	116 kWh	0.6	0.4	8.1	2.6
C	161 kWh	0.8	0.5	11.3	3.5
D	210 kWh	1.1	0.7	14.7	4.6
E	255 kWh	1.3	0.9	17.9	5.6

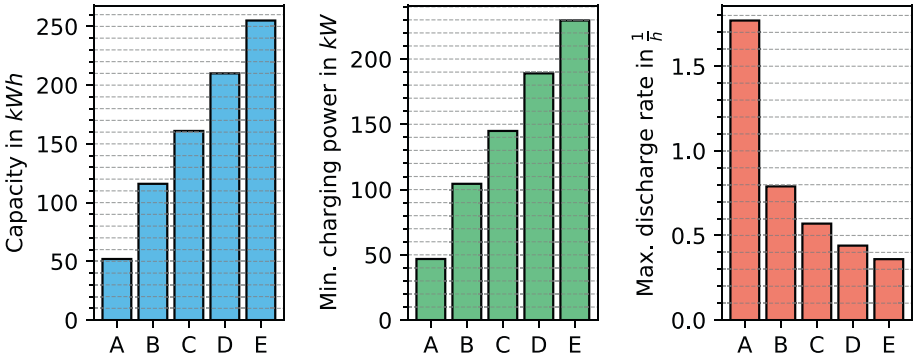

Fig. 11. Capacity, charging power and C-rates for discharging for thermal storage systems in the reference vehicle in scenario A to E.

this case, hybrid OESS were defined for the scenarios A to E with a same overall weight. The thermal storage capacity from the scenario is the amount of battery capacity replaced. The rest of the hybrid OESS capacity is filled with batteries to reach the same weight for all scenarios. The results in Table 4 show that between 1.1 % and 5.6 % additional energy can be stored in this hybrid OESS. The capacity in the energy storage can be seen as proportional to the range of the vehicle. For current BEMUs, the range is between 80 km and 120 km according to section 1.1, which would lead to an increase of range by 7 km with the hybrid OESS. For the scenario presented in Fig. 5, the range is 236 km, so the increase in energy would lead up to additional 13 km of vehicle range. This increase expands the flexibility of the vehicles in daily operation and makes them more resilient against disturbances. In addition, the overall cost of the hybrid OESS are lower than the battery OESS, as the specific cost of the thermal storages are lower.

4. Discussion

The presented results show that thermal storages can be used to increase the amount of energy stored in the OESS and therefore also the range of battery electric rail vehicles. For the investigation, including the modeling of the thermal car body, several assumptions where made. These assumptions are discussed in combination with uncertainties and weaknesses of the methodical approach in this chapter. Subsequently, the chosen scenario, lessons learned and potential future work is discussed.

The thermal power demand of HVAC, simulated with the TCBM, was calculated based on stationary OPs as the temperature, humidity, passenger rate and radiation were not varied in the simulation, which represents an uncertainty in the methodical approach. Unsteady conditions were applied by the change in vehicle velocity and therefore heat transfer coefficients. Vehicles in passenger operation experience unsteady conditions in all the parameters stated before. Measurement data from battery electric rail vehicles in operation show therefore a different behavior than the steady points used for simulation model parametrization. Nevertheless, the overall energy demand was validated, which indicates minor effects of this unsteadiness on the energy demand calculation. For the evaluation of weight, volume and cost, potential constant values of energy density for the energy storage system were applied. As the energy density varies with system design, these values will change with further improvement in the technology. The methodical approach can be strengthened if the energy density as well as the weight and cost of a demonstrator system as experimental setup is taken as input parameters in the future. Nevertheless, for an analysis of requirements, the applied energy densities for the energy storage define clearly the potential of the thermal storages in BEMU application. For the presented analysis, the assumption of electrical charging of the thermal storage was taken. A thermal charging based on waste heat of the battery and the DCDC of the rail vehicle was not suitable as the temperature level of dissipated heat is low. Also, the amount of waste heat was not enough to provide the energy demand in all OPs, which leads to the fact that an electrical charging of the thermal storage is necessary.

The presented work studies the track scenario from Linköping to Kalmar with a distance of 236 km. For BEMU application, this distance is above average as current vehicles have a range between 80 km and 120 km. Therefore, for the sizing of the thermal storage, this scenario represents a maximum in thermal capacity. The developed methodology of the sizing of the hybrid OESS with a thermal storage and a battery can be applied to any track scenario, independent of the distance. Improvement in capacity of the OESS can be expected also for scenarios with lower distance, even though the effect of increased range is higher at long distances.

In future work, the configuration of a hybrid OESS with battery and thermal storage can be defined with the developed methodical approach for any track, time table and vehicle configuration. The sizing of the thermal storage module can be applied to the specific use cases. Alternatively, a large number of scenarios can be simulated and standardized module sizes can be concluded. Also, the results of this work can be transferred to other fields if scenarios from other vehicle platforms, like buses are included in this evaluation. With standardized intermodal module sizes, the cost for the thermal energy storage can be reduced further as economies of scale occur with mass production of those sizes. Technology readiness level of the thermal storage system is low at the moment, as the technology is not applied in rail vehicles yet. For application in the future, further research, development and demonstration are necessary to define energy density for different module sizes and to increase the technology readiness level. An experimental setup of a thermal storage system demonstrator in lab environment with a rail specific module size would lead to such an increase in technology readiness level. A demonstrator makes it possible to study the complexity of operation of a thermal storage with metallic storage material as they require high temperatures in the overall system. Challenges in the implementation of a demonstrator lie especially in the system design. Chemical compatibility of the housing and the thermal storage material must be given to avoid corrosion in operation. In general, the high operating temperatures of up to 700 °C represent a challenge for the demonstrator design as thermal insulation needs to fulfill rail-specific safety requirements in this temperature range. Also, the thermal resistances from the thermal charging system and the heat exchangers of the discharging systems to the storage material are key performance indicators. They must be as low as possible to avoid high temperature differences to charge or discharge the system. Another challenge for the experimental setup is the mechanical and thermal stability as high temperature differences between inside and outside of the thermal system lead to mechanical stress of the material, which needs to be considered in the design process.

Future work with system simulations could address the development of operational concepts for rail vehicles with thermal storages. In there, operational effects like the removal of thermal storages during summer months and the re-installation in winter months can be evaluated. The combination of thermal storage systems with heat pumps is also to be investigated. Heat pumps have a low COP or are no longer functional at very low ambient temperatures. Thermal storage systems could cover heating demand at these operating points, so that a combination of both technologies could be advantageous for battery trains. In addition, system simulations can investigate the defined module sizes with an onboard vehicle energy management. In there, the explicit effects on battery storage can be studied to quantify the decreased degradation. An energy management strategy which defines charging and discharging times for thermal storage and battery in operation can be developed to optimize overall system efficiency and degradation. For battery electric rail vehicles, especially the change in catenary availability during the operation is one boundary conditions for the charging strategy. The reduced degradation through optimized energy management strategy with thermal storage application is one key aspect to reduce cost in the OESS of battery electric rail vehicles. Batteries will likely be replaced several times during the lifetime of the vehicles, as the rail vehicles are often designed for 30 years. A reduced degradation leads to less replacements of the battery in the vehicle life and therefore to reduced costs.

Overall, lessons learned from this study are that thermal storages are a suitable energy storage for battery electric rail vehicles, especially if the vehicles operate in climate zones with a high demand for heating. In those use cases, thermal storage systems as part of a hybrid OESS with batteries can reduce the cost and increase vehicle range and flexibility.

5. Conclusion

Battery electric multiple units currently enable a range of around 100 km in operation. The presented study investigates an application in northern Europe with a track length of 236 km and how thermal storages

can help to enable battery electric vehicles to perform in this scenario under all expected environmental conditions.

A thermal car body model in Python is set up, validated and used to define the requirement of thermal storage in a battery electric rail vehicle. The thermal power demand for HVAC is calculated with 48 kW in the most demanding cooling case and with 92 kW in the most demanding heating case. Based on this, a thermal storage capacity between 52 kWh and 255 kWh is calculated, depending on the sizing scenario. The maximum discharge power of 92 kW for the thermal storage corresponds to maximum C-rates for discharging between 0.38 1/h and 1.8 1/h. The charging process with a C-rate of 0.9 1/h corresponds to an average charging rate for the thermal storage between 48 kWh and 230 kW. Overall, the thermal storage adds up to 5.6 % of additional energy to the OESS compared to a stand-alone battery storage system with equivalent weight. The thermal capacity, as well as the discharging and charging rates, represent the energetic requirements of the thermal storage, which define the sizing of the system. The developed methodical approach of the sizing based on the thermal energy demand for HVAC can be applied to a wide range of operational scenarios of battery-electric rail vehicles. Especially in climate zone III, with a high energy demand for heating, benefits of thermal storage apply. But also, in climate zone I a significant energy demand for heating is presented, indicating that also in there an application is beneficial.

Overall, the presented results show that the application of thermal storages in the energy storage of battery electric rail vehicles reduces the cost and increases range and flexibility of the vehicles during the operation. For operators of these vehicles, these effects lead to an efficient and low-emission public rail transport.

Funding statement

Funded by the European Union. Views and opinion expressed are however those of the author(s) only and do not necessarily reflect those of the European Union or the Europe's Rail Joint Undertaking. Neither the European Union nor the granting authority can be held responsible for them. The project FP4 – Rail4EARTH is supported by the Europe's Rail Joint Undertaking and its members.

CRediT authorship contribution statement

Steffen Wieser: Writing – original draft, Visualization, Validation, Supervision, Software, Methodology, Investigation, Formal analysis, Conceptualization. **Lucas Naveau:** Writing – original draft, Visualization, Validation, Software, Methodology. **Werner Kraft:** Writing – review & editing. **Ruth Arregi Beristain:** Writing – review & editing, Investigation. **Armando Anson:** Writing – review & editing, Investigation.

Declaration of competing interest

The authors declare that they have no known competing financial interests or personal relationships that could have appeared to influence the work reported in this paper.

Data availability

Data will be made available on request.

References

[1] Eurostat, "Length of railway lines by number of tracks and electrification of lines," 2023, doi: 10.2908/RAIL_IF_LINE_TR.
[2] Chamaret A, Mannevy P, Clément P, Ernst J, Flerlage H. Analysis, trends and expectations for low carbon railway". Transp Res Procedia 2023;72:2684–91. https://doi.org/10.1016/j.trpro.2023.11.808.
[3] Boev P, Zimmermann U, Ebrecht B, von Mach S. First Passenger Operation of a State-of-the-art Battery-Electric Multiple Unit (BEMU) in Germany. Transp Res Procedia 2023;72:2510–7. https://doi.org/10.1016/j.trpro.2023.11.757.
[4] S. Herwartz-Polster, J. Pagenkopf, J. Kaiser, and M. Freienhofer, "Power Forecast of Overhead Catenary Islands in Battery Electric Train Operation: Case Study of Pfalznetz," in Proceedings of the Sixth International Conference on Railway Technology: Research, Development and Maintenance, Prague, Czech Republic, J. Pombo, Ed., 2024, pp. 1–14, doi: 10.4203/ccc.7.12.4.
[5] Pugi L, Di Carlo L. Multi-modal battery-operated trains on partially electrified lines: A case study on some regional lines in Italy. Proceedings of the Institution of Mechanical Engineers, Part F: Journal of Rail and Rapid Transit 2024;238(7): 873–85. https://doi.org/10.1177/09544097241234959.
[6] Herwartz-Polster S, Böhm M, Stickel S, Streuling C, Hertel B, Pagenkopf J. "Applications – Transportation Applications | Rail Vehicles - Fuel Cells and Batteries," in Encyclopedia of electrochemical power sources. J. Garche 2025: 268–79. https://doi.org/10.1016/B978-0-323-96022-9.00051-7.
[7] Fedele E, Iannuzzi D, Del Pizzo A. Onboard energy storage in rail transport: Review of real applications and techno-economic assessments. IET Electrical Syst in Trans 2021;11(4):279–309. https://doi.org/10.1049/els2.12026.
[8] González-Gil A, Palacin R, Batty P, Powell JP. A systems approach to reduce urban rail energy consumption. Energ Conver Manage 2014;80:509–24. https://doi.org/10.1016/j.enconman.2014.01.060.
[9] M. Schenker and F. Kuhlkamp, "Optimization Model for Operation of Battery Multiple Units on Partly Electrified Railway Lines," in 2021 Sixteenth International Conference on Ecological Vehicles and Renewable Energies (EVER), Monte-Carlo, Monaco, 2021, pp. 1–8, doi: 10.1109/EVER52347.2021.9456608.
[10] Schenker M, Schirmer T, Dittus H. Application and improvement of a direct method optimization approach for battery electric railway vehicle operation. Proceedings of the Institution of Mechanical Engineers, Part F: Journal of Rail and Rapid Transit 2021;235(7):854–65. https://doi.org/10.1177/0954409720970002.
[11] Dullinger C, Struckl W, Kozek M. Holistic energy simulation and optimization tool for urban rail vehicles. Energ Conver Manage 2018;174:101–11. https://doi.org/10.1016/j.enconman.2018.08.036.
[12] Streuling C, Pagenkopf J, Schenker M, Lakeit K. Techno-Economic Assessment of Battery Electric Trains and Recharging Infrastructure Alternatives Integrating Adjacent Renewable Energy Sources. Sustainability 2021;13(15):8234. https://doi.org/10.3390/su13158234.
[13] Kapetanović M, Núñez A, van Oort N, Goverde RM. Energy use and greenhouse gas emissions of traction alternatives for regional railways. Energ Conver Manage 2024;303:118202. https://doi.org/10.1016/j.enconman.2024.118202.
[14] González-Gil A, Palacin R, Batty P. Optimal energy management of urban rail systems: Key performance indicators. Energ Conver Manage 2015;90:282–91. https://doi.org/10.1016/j.enconman.2014.11.035.
[15] Seo J, Vijayagopal R, Kim N, Rousseau A, Stutenberg K. Effects of ambient temperature on electric vehicle range considering battery Performance, powertrain Efficiency, and HVAC load. Energ Conver Manage 2025;326:119493. https://doi.org/10.1016/j.enconman.2025.119493.
[16] DIN EN 14750:2025-02, Railway applications - Air conditioning for urban, suburban and regional rolling stock - Comfort parameters and type tests; German version EN 14750:2024, Berlin.
[17] DIN EN 13129:2016-12, Bahnanwendungen_- Luftbehandlung in Schienenfahrzeugen des Fernverkehrs_- Behaglichkeitsparameter und Typprüfungen; Deutsche Fassung EN_13129:2016, Berlin.
[18] DIN EN 50591:2019-12, Railway Applications - Rolling Stock - Specification and verification of energy consumption; German version EN 50591:2019.
[19] Widmer F, van Dooren S, Onder CH. Optimization of the energy-comfort trade-off of HVAC systems in electric city buses based on a steady-state model. Control Eng Pract 2025;154:106158. https://doi.org/10.1016/j.conengprac.2024.106158.
[20] Hofstädter RN, Zero T, Dullinger C, Richter G, Kozek M. Heat capacity and heat transfer coefficient estimation for a dynamic thermal model of rail vehicles. Math Comput Model Dyn Syst 2017;23(5):439–52. https://doi.org/10.1080/13873954.2016.1263670.
[21] Haddad RA, Mansour C, Kim N, Seo J, Stutenberg K, Nemer M. Comparative analysis of thermal management systems in electric vehicles at extreme weather conditions: Case study on Nissan Leaf 2019 Plus, Chevrolet Bolt 2020 and Tesla Model 3 2020. Energ Conver Manage 2025;332:119706. https://doi.org/10.1016/j.enconman.2025.119706.
[22] Schmeling D, Bosbach J. Influence of shape and heat release of thermal passenger manikins on the performance of displacement ventilation in a train compartment. Indoor Built Environ 2020;29(6):835–50. https://doi.org/10.1177/1420326X19856673.
[23] Ma J, Liu A, Zhang P, Chen Y, Cai Y. Collaborative thermal management of power battery and passenger cabin for energy efficiency optimization. Energ Conver Manage 2023;293:117514. https://doi.org/10.1016/j.enconman.2023.117514.
[24] Wu Y, et al. Integrated battery thermal and energy management for electric vehicles with hybrid energy storage system: A hierarchical approach. Energ Conver Manage 2024;317:118853. https://doi.org/10.1016/j.enconman.2024.118853.
[25] Zhang N, Lu Y, Kadam S, Yu Z. Investigation of the integrated fuel cell, battery, and heat pump energy systems. Energ Conver Manage 2023;276:116503. https://doi.org/10.1016/j.enconman.2022.116503.
[26] Li K, et al. Assessment method of the integrated thermal management system for electric vehicles with related experimental validation. Energ Conver Manage 2023;276:116571. https://doi.org/10.1016/j.enconman.2022.116571.
[27] Liu X-A, Zhang F, Zhang Z, Huang Y, Chen L, Li X. A three-heat source segmented heating control strategy based on waste heat recovery technology for electric

vehicles. Energ Conver Manage 2024;300:117932. https://doi.org/10.1016/j.enconman.2023.117932.
[28] Hu Z, Qiu D, Zhao J, Peng X, Peng H. Integrated design of multi-circuit thermal management system with battery waste heat utilization for new energy vehicle and performance assessment. Energ Conver Manage 2024;312:118566. https://doi.org/10.1016/j.enconman.2024.118566.
[29] E. Trygstad, "R744 HVAC unit for NSB Flirt trains," 2019. [Online]. Available: https://ntnuopen.ntnu.no/ntnu-xmlui/handle/11250/2454941.
[30] Jiang F, Wang Y, Yu B, Wang D, Shi J, Chen J. Effects of various operating conditions on the performance of a CO2 air conditioning system for trains. Int J Refrig 2019;107:105–13. https://doi.org/10.1016/j.ijrefrig.2019.07.009.
[31] Kwon S, Lee D, Ham SH, Lee M, Kim Y. Performance comparison of thermal management systems for electric vehicles using single- and dual-loop indirect heat pumps with propane. Energ Conver Manage 2025;327:119535. https://doi.org/10.1016/j.enconman.2025.119535.
[32] Liu W, Deng Q, Huang W, Liu R. Variation in cooling load of a moving air-conditioned train compartment under the effects of ambient conditions and body thermal storage. Appl Therm Eng 2011;31(6–7):1150–62. https://doi.org/10.1016/j.applthermaleng.2010.12.010.
[33] Xu Z, Zhao N, Yan Y, Gao S, Hillmansen S. Electric-thermal collaborative system and control for hydrogen-fuel cell passenger trains in the UK's winter. Energ Conver Manage 2025;328:119629. https://doi.org/10.1016/j.enconman.2025.119629.
[34] Deng L, Li S, Tang X, Yang K, Lin X. Battery thermal- and cabin comfort-aware collaborative energy management for plug-in fuel cell electric vehicles based on the soft actor-critic algorithm. Energ Conver Manage 2023;283:116889. https://doi.org/10.1016/j.enconman.2023.116889.
[35] Broatch A, Olmeda P, Margot X, Aceros S. Different strategies in an integrated thermal management system of a fuel cell electric bus under real driving cycles in winter. Energ Conver Manage 2023;288:117137. https://doi.org/10.1016/j.enconman.2023.117137.
[36] M. Kordel, M. M. Heeland, and K. Knetsch, "IRSA 2023 Proceedings: Waste Energy AC Technologies in H2-Multiple Units," 2024, doi: 10.18154/RWTH-2024-00257.
[37] Jiangzhou S, Wang RZ, Lu YZ, Xu YX, Wu JY. Experimental study on locomotive driver cabin adsorption air conditioning prototype machine. Energ Conver Manage 2005;46(9–10):1655–65. https://doi.org/10.1016/j.enconman.2004.07.008.
[38] Wieser S, Schenker M, Schwurack H, Hoffmann F, Donner S, Konrad M. Efficient Air Conditioning of Battery-Electric Multiple Units (BEMU): Modeling and Optimization. In: McNally C, Carroll P, Martinez-Pastor B, Ghosh B, Efthymiou M, Valantasis-Kanellos N, editors. Transport Transitions: Advancing Sustainable and Inclusive Mobility (Lecture Notes in Mobility). Cham: Springer Nature Switzerland; 2025. p. 485–91.
[39] J. Lidén, "Optimization of comfort-related energy and thermal comfort for commuter trains: A case study of Stockholm commuter trains," 2023. [Online]. Available: http://kth.diva-portal.org/smash/record.jsf?pid=diva2%3A1798585&dswid=-9168.
[40] Lu P, et al. Thermodynamic analysis and evaluation of a novel composition adjustable Carnot battery under variable operating scenarios. Energ Conver Manage 2022;269:116117. https://doi.org/10.1016/j.enconman.2022.116117.
[41] Chen H, Jia X, Wang H, Ning Y, Li X, Duanmu L. Optimization and evaluation of a near-zero carbon energy system: Integration of photovoltaics, heat pumps, and combined thermal and electrical storage solutions. Energy Conversion and Management 2025;327:119583. https://doi.org/10.1016/j.enconman.2025.119583.
[42] Laterre A, Dumont O, Lemort V, Contino F. Is waste heat recovery a promising avenue for the Carnot battery? Techno-economic optimisation of an electric booster-assisted Carnot battery integrated into different data centres. Energ Conver Manage 2024;301:118030. https://doi.org/10.1016/j.enconman.2023.118030.
[43] Ge G, Cai X, Sun H, Zhang Y, Wang H, Li R. Optimization design of an adiabatic compressed air energy storage system with sliding pressure operation and packed bed thermal energy storage based on a one-dimensional loss model. Energ Conver Manage 2025;328:119626. https://doi.org/10.1016/j.enconman.2025.119626.
[44] Yin S, Bai C, Zheng K, Zhang Y, Yan X, Liu Z. Geothermal energy-assisted pumped thermal energy storage: Configuration mapping. Energ Conver Manage 2025;329:119660. https://doi.org/10.1016/j.enconman.2025.119660.
[45] Wilks M, Wang C, Ling-Chin J, Wang X, Bao H. Thermochemical energy storage for cabin heating in battery powered electric vehicles. Energ Conver Manage 2023;291:117325. https://doi.org/10.1016/j.enconman.2023.117325.
[46] W. Kraft, V. Jilg, M. Klein Altstedde, T. Lanz, P. Vetter, and D. Schwarz, "Thermal High Performance Storages for Use in Vehicle Applications," in Energy and Thermal Management, Air-Conditioning, and Waste Heat Utilization: 2nd ETA Conference, November 22-23, 2018, Berlin, Germany, C. Junior, Ed., Cham: Springer International Publishing AG, 2019, pp. 66–79.
[47] Kraft W, Stahl V, Vetter P. Thermal Storage Using Metallic Phase Change Materials for Bus Heating—State of the Art of Electric Buses and Requirements for the Storage System. Energies 2020;13(11):3023. https://doi.org/10.3390/en13113023.
[48] J. Buschbeck, S. Yang, S. von Mach, S. Donner, and W. Kraft, "Thermische Hochleistungsspeicher für batterieelektrische Schienenfahrzeuge," 2022. [Online]. Available: https://www.zevrail.de/artikel/thermische-hochleistungsspeicher-fuer-batterieelektrische-schienenfahrzeuge.
[49] Rawson AJ, Kraft W, Gläsel T, Kargl F. Selection of compatible metallic phase change materials and containers for thermal storage applications. J Storage Mater 2020;32:101927. https://doi.org/10.1016/j.est.2020.101927.
[50] Bellos E. Thermodynamic analysis of a Carnot battery unit with double exploitation of a waste heat source. Energ Conver Manage 2024;299:117844. https://doi.org/10.1016/j.enconman.2023.117844.
[51] W. Kraft, F. Nees, V. Stahl, and P. Vetter, "Thermal High Performance Storages for electric bus heating - overview on the current state of development," 2021. [Online]. Available: https://elib.dlr.de/142821/.
[52] Kuchling H. Taschenbuch der Physik: Mit Tabellen. 20th ed. München: Fachbuchverl. Leipzig im Carl Hanser Verl; 2011.
[53] Trafikverket, "Regeringsuppdrag Delelektrifiering - Government mission partial electrification," 2024. [Online]. Available: https://trafikverket.diva-portal.org/smash/get/diva2:1850342/FULLTEXT01.pdf.
[54] Meteostat, "Weather Station Kalmar Airport," 2025. [Online]. Available: https://meteostat.net/en/place/se/kalmar.
[55] S. Donner, I. Elola, and H. Dittus, "Validation of a BEMU Thermal Car Body Model for the Shift2Rail Project FINE-2," 2022, doi: 10.18154/RWTH-2022-01843.
[56] S. Donner, M. Schenker, M. Konrad, H. Dittus, and N. Schindler, "Shift2Rail FINE-2 - Deliverable D4.3 - Study on potential energy savings by new concepts and smart control of HVAC systems," 2022. [Online]. Available: https://projects.shift2rail.org/download.aspx?id=75874bb6-a8c8-4b09-8946-1b0d5dbdade0.